Chemical Engineering Journal 166 (2011) 384–390

Contents lists available at ScienceDirect

Chemical Engineering Journal

journal homepage: www.elsevier.com/locate/cej

Synthesis and characterization of microcapsules containing Rubitherm®RT27 obtained by spray drying

A.M. Borreguero[a], J.L. Valverde[a], J.F. Rodríguez[a], A.H. Barber[b], J.J. Cubillo[c], M. Carmona[a,*]

[a] Department of Chemical Engineering, University of Castilla – La Mancha, Av. Camilo José Cela s/n, 13004 Ciudad Real, Spain
[b] Department of Materials, School of Engineering and Materials Science, Queen Mary University of London, Mile End Road, E1 4NS London, UK
[c] Acciona Infraestructuras S.A., C/Valportillo II, 8, 28108 Alcobendas, Spain

ARTICLE INFO

Article history:
Received 2 July 2010
Received in revised form 4 October 2010
Accepted 20 October 2010

Keywords:
Microcapsules
Paraffin waxes
Carbon nanofibers
Energy storage
Thermal comfort

ABSTRACT

Spray drying was used to encapsulate the paraffin Rubitherm®RT27 with and without carbon nanofibers (CNFs) showing a microencapsulation yield of 63%. Characteristics of microcapsules containing this phase change material (PCM) were dependent on the location in which they were collected in the spray dryer. The mechanical properties of the above-mentioned materials were studied by atomic force microscopy (AFM) indicating that the force required to produce the same microcapsule deformation was approximately 183% higher when 2 wt% of CNFs was added in the microcapsule recipe. The thermal energy storage (TES) capacity of the obtained microcapsules (98.1 J/g) was similar to those exhibited by microcapsules produced by a suspension polymerization technique using styrene as shell material (96.7 J/g) and that of a commercial material (116.2 J/g). In the same way, the CNF content maintained the TES capacity of the microcapsules (95.6 J/g) and seemed to enhance their thermal conductivity. Finally, the stability studies of the synthesized material carried out during 3000 cycles indicated that the developed material was stable and worked in reversible way.

1. Introduction

Phase change materials (PCMs) are extensively used for storing and releasing thermal energy by taking advantage of their high heats of fusion, being applied in textiles, buildings, medical therapies, packaging and space aircraft [1,2]. Paraffin waxes, eutectic materials, salt mixtures and salt hydrates are the most commonly used PCMs [3,4]. Organic materials present a number of advantages over inorganics; they have high chemical and thermal stability and do not exhibit segregation, supercooling or corrosion problems. Paraffin waxes are the most common organic PCMs used due to their large latent heat or TES capacity, abundance, low cost and their adjustable melting point [5]. Therefore, they are a candidate for building materials where heat can be absorbed during daytime, providing thermal insulation, and released at colder times at nighttime. However, the containment of paraffin wax, its interaction with the surrounding environment and leakage in the liquid state make direct use in building constructions difficult [6], although a stable composite has been found by Sari et al. [7] when lauric acid was incorporated by vacuum impregnation into expanded perlite.

Microencapsulation of PCMs with a polymeric shell is considered to be one of the best technical options for containment of the paraffin wax for incorporation into a building structure [5]. The confinement of waxes into microcapsules allowed to increase the heat-transfer area and control the volume changes as the phase change occurs [8]. Different polymers, such as polystyrene (PS) [9–11], styrene-methyl metacrylte copolymer [12], melamine-formaldehyde [13–16], polyurea [17] and urea-formaldehyde [18] have been used as the polymer shell, and mixtures of polyethylene polymer and ethylvinylacetate copolymer (EVA) have been used as the supporting material of paraffin waxes [19–21] in which the vinylacetate group makes the long chain of the polymers more compatible with the short ones of the paraffin waxes and improves the mechanical properties of the paraffin–polymer compounds [22].

The most common methods described in the literature for microencapsulation are interfacial polymerization, emulsion polymerization, suspension polymerization, coacervation and spray drying [8–10,14,18,23,24].

In previous works, PCMs were successfully encapsulated by the chemical process suspension polymerization technique using PS as the polymer shell. In that process was found that the amount and yield of the core microencapsulation was strongly affected by the core/shell mass ratio [10–12].

The above-mentioned chemical methods involve the use of many reagents (surfactants, inhibitors, initiators, monomers, etc.) that can be found in the liquid phase, increasing the cost of the waste stream treatment, besides the particle size is really difficult to be controlled requiring the use of a Shirasu porous glass (SPG)

* Corresponding author. Tel.: +34 902204100; fax: +34 926295318.
E-mail address: Manuel.CFranco@uclm.es (M. Carmona).

1385-8947/$ – see front matter © 2010 Elsevier B.V. All rights reserved.
doi:10.1016/j.cej.2010.10.055

membrane with a specific pores size [9,10]. On the other hand, spray drying technique minimizes the waste generation and the loss of the raw material, allowing the manufacture of a homogeneous product with a desired particle size distribution depending on the atomizer design [25,26]. Furthermore, this process can be easily controlled and scaled-up [27].

In this paper, the ability to produce microcapsules containing a commercial wax, using a low density polyethylene (LDPE) and ethylvinylacetate copolymer (EVA) as the shell materials by the physical technique of spray drying is studied. The similarity of the chemical structure of polyethylene and EVA with the paraffin makes these materials particularly effective as a shell material. Besides, these materials have low density, are versatile, inexpensive, and they do not interact with the surrounding environment and the building materials. The selected commercial wax was the Rubitherm®RT27 attending to the suggestions of Peippo et al. [28] who stated that in order to get an optimum thermal energy storage in buildings, the melting point of the used PCM should be three degrees higher than the average room temperature.

The spray drying technique involves the atomization of a homogeneous liquid stream (solution, suspension or paste) in a drying chamber where the solvent is evaporated and solid particles are obtained [27]. This technique is suitable for heat-sensitive materials and has been applied in the microencapsulation of food and pharmaceutical materials as well as in the ceramic and painting industries [25,27,29–31]. However, only the production of microcapsules constituted by a paraffin wax in gelatin-acacia and octadecane in titania have been reported in the literature with this technique [8,32] reporting high core loading even higher than 80% with a homogeneous particle size within 0.1–5 μm and microencapsulation efficiencies between 60 and 92%. According to these results, this technique seems to be better than those aforementioned. Thus, the microencapsulation of a commercial wax, Rubitherm®RT27, using a low density polyethylene (LDPE) and ethylvinylacetate copolymer (EVA) as shell materials was accomplished by the physical technique of spray drying and reported in this paper. Besides, the production of microcapsules with enhanced thermal and mechanical properties is typically achieved by further incorporation of metallic additives within the microcapsule structure [4,5,33–36]. In this work, carbon nanofibers are explored as additives to improve the thermal and mechanical properties of the microcapsules.

Hence, the aim of this work is to synthesize and characterize the microcapsules obtained by a spray drying technique, containing Rubitherm®RT27 with and without CNFs, and compare their properties with other microencapsulated PCMs. Finally, the thermal stability of synthesized microcapsules obtained by spray drying without CNFs and by suspension polymerization is studied.

2. Materials and methods

2.1. Materials

Four types of microcapsules containing PCMs were used: commercial microcapsules supplied by BASF, called Micronal®DS 5001X; microcapsules containing paraffin wax Rubitherm®RT27 with and without carbon nanofibers, obtained by spray drying, and microcapsules containing Rubitherm®RT27 synthesized by suspension polymerization, following the recipe described by Sanchez et al. [9] whose thermal properties and the particle size distribution have been reported in a previous work [11]. Carbon nanofibers were synthesized as described by Jiménez et al. [37].

2.2. Microcapsules synthesis by means of spray drying

The spray dryer experimental device is shown in Fig. 1. A homogeneous liquid solution (*feed stream*) was atomized by means of a carrier gas stream (*compressed* N_2). Following atomization, the sol-

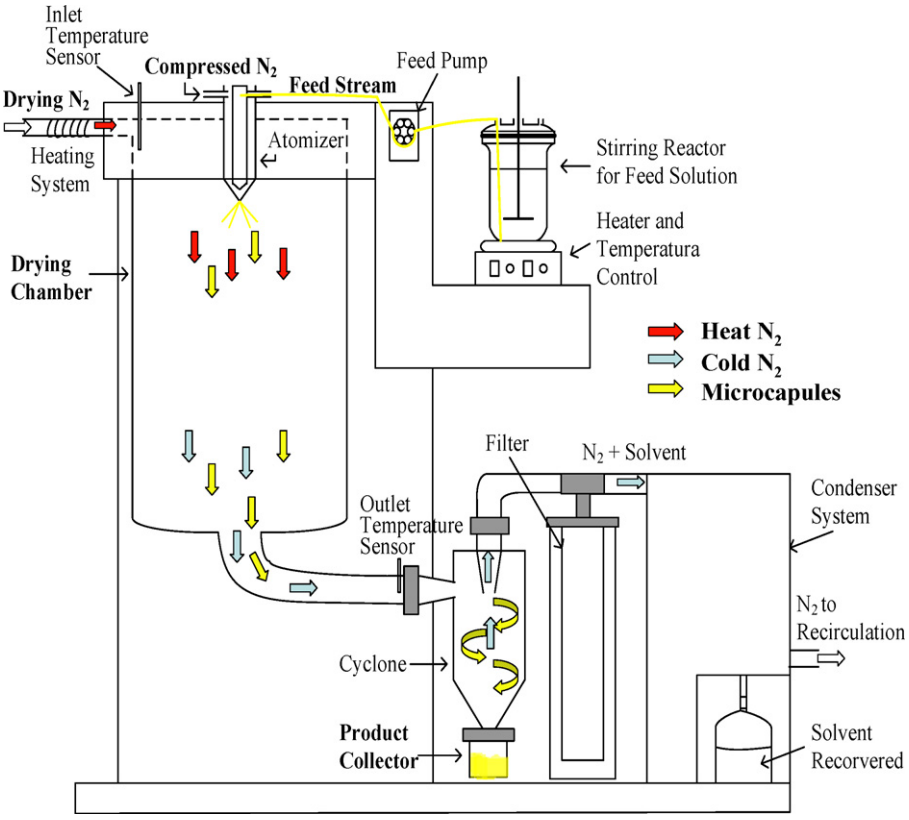

Fig. 1. Schematic representation of the spray drying equipment.

vent was evaporated and the particles were dried by an additional nitrogen stream (*drying* N_2) in the *drying chamber*. The final product was recovered in the *collector*.

The used spray dryer was a Büchi-290 and the operating conditions and formulation used to obtain the microcapsules containing the PCMs can be found in the European patent EP2119498 (A1) [38]. Results obtained at lab scale indicated that a 63 wt% of the fed solid materials were transformed into microcapsules and the non-encapsulated ones were recovered and recycled to the process. Besides, with the aim of enhancing the thermal conductivity of the microcapsules, CNFs were uniformly distributed in the feed stream and the used weight percentage (2 wt%) is in the range of those reported in the literature [39].

2.3. Scanning electron microscopy (SEM)

Particle size and morphology of the microcapsules were observed by means of a FEI QUANTA 200 scanning electron microscope at Acciona Technological Centre in Madrid and the average particle size was determined by using the commercial program Motic Images Plus.

2.4. Atomic force microscopy (AFM)

The mechanical properties of individual microcapsules were measured by using atomic force microscopy (AFM). Microcapsules with an average diameter of 5 μm were fixed to a commercial adhesive (Poxipol®, Arg.) for mechanical testing. An AFM (NTegra, NT-MDT, Rus) was used to image the sample and locate the microcapsules using semicontact imaging. Mechanical testing of an individual microcapsule was carried out according to previous mechanical testing procedures [40]. Briefly, the AFM probe was brought into contact with an isolated microcapsule on the substrate surface (defined as the zero point of the microcapsule deflection axis) followed by a defined extension of the AFM *Z*-piezo to push the probe into the microcapsule and also resulted in bending of the AFM cantilever attached to the AFM probe. The recorded cantilever bending is converted to force by knowing the spring constant k of the cantilever, with $k = 7.7$ N/m using the Sader calibration method. Thus, the cantilever deflection was converted to applied force by means of the spring constant, $F = k\Delta$. The microcapsule deformation δ was calculated using $\delta = (Z - Z_0) - \Delta$, where Z is the absolute Z-piezo extension; Z_0 is the initial Z-piezo extension upon the probe contact; and Δ is the bending of the cantilever at Z [40]. The total deformation behavior of an individual microcapsule was recorded continually with increasing applied force to give resultant force–displacement curves. This procedure was done five times to check the reproducibility of the experiments, selecting microcapsules of the same particle size.

2.5. Differential scanning calorimetry (DSC)

A differential scanning calorimeter (DSC, Q100 TA Instruments, USA) was used for the latent heat determination of paraffin Rubitherm®RT27 and microcapsules. These analyses were done using N_2 as carrier gas at a volume flow of 50 ml/min, a fixed sample mass of 6.0 mg and aluminum pans. Measurements of the latent heat were performed varying the temperature in the range from −30 to 50 °C using a heating rate of 5 °C/min at which the thermal equilibrium is established. In order to check the influence of the thermal conductivity on the heat absorption, further DSC analyses were performed by using a heating rate of 30 °C/min, condition that provides less accurate results due to the low thermal conductivity and high melting enthalpy of the PCM, since it is more complicated to achieve the thermal equilibrium [41]. Each microcapsules type was analyzed at least three times and the average value was taken as the latent heat of the sample. In order to avoid the effect of the sample size on the latent heat or in the melting point, samples having the same weight were analyzed.

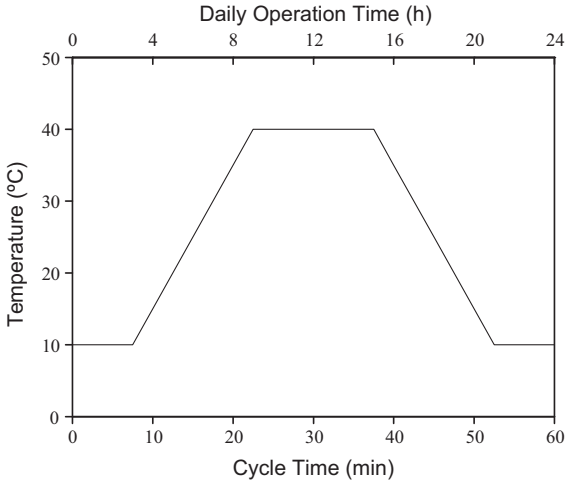

Fig. 2. Thermal cycle representing one operation day.

2.6. Microcapsules stability

Microcapsules thermal stability studies were carried out using a climatic chamber (Heraeus Vötsch HC4015) at a constant relative humidity of 65%, equipped with a K-type thermocouple in the middle. In this chamber, glass vials containing 5 g of microcapsules contacting with K-type thermocouple were placed. The accuracy of temperature measurements was 0.1 °C. Microcapsules were subjected to several thermal cycles, changing successively the climatic chamber temperature above and under the paraffin melting point. Each cycle corresponds with a typical Madrid summer's day. The total cycles of analysis were 3000 which are equivalent with 30 operating years. The thermal stability cycle is shown in Fig. 2.

The aim of this treatment is to check the reversibility of the energy storage by means of the microencapsulated Rubitherm®RT27 when it works for at least 30 years and that no paraffin leakage takes place from the microcapsules when it was melted.

3. Results and discussion

3.1. Particle size and morphology

Fig. 3 shows SEM micrographs of the microcapsules containing Rubitherm®RT27 collected at different locations in the spray drying equipment. The microcapsules obtained in the collection vessel (Fig. 3a) have a more homogeneous and defined spherical shape than those obtained inside the drying chamber (Fig. 3b) which seem to agglomerate together. The microcapsule particle size both in the collection vessel and drying chamber was typically smaller than 10 μm, having the collector product an average particle size of 3.9 μm according to the Motic Images Plus program while particles collected in the drying chamber appear to be bound together by melted polymer. The particle agglomeration in the chamber can be due to liquid polymer bridges that can be formed and solidified between two or more spray droplets [42]. As the sprayed polymer shell materials of LDPE and EVA are thermoplastics [43], taking into account that 110 °C is the inlet gas temperature which is close to the melting point of the LDPE ranging between 105 and 115 °C and really higher than that of EVA located from 85 to 90 °C (according to the manufacturer datasheet), these material can be

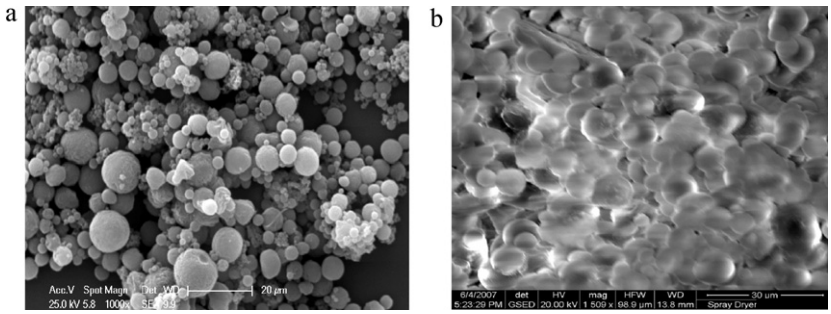

Fig. 3. SEM images of microcapsules of LDPE–EVA containing Rubitherm®RT27 and CNFs, with magnification of a) collection vessel, operating at 25 kV and with magnification ×1000 and b) drying chamber, operating at 20 kV and with magnification ×1500.

found molten into the chamber bridging the microcapsules and promoting the agglomeration. Nevertheless, these materials solidify entirely inside the chamber because the outlet temperature was only 62 °C. As expected, the increased weight of the agglomerated material lowers the transport efficiency of the material to the collector by the carrier gas. The chamber product could be minimized by cooling the drying chamber wall where the solvent evaporates or using a higher carrier gas flow [44]. Thus, the final product should be mainly obtained in the collection vessel.

Fig. 4 shows the morphology of the microcapsules when a 2 wt% of CNFs were added to the feed stream. Fig. 4a shows that when CNFs were incorporated, the particles tend to be more agglomerated than those produced without CNFs, increasing their particle size, widening the particle size distribution and promoting non-spherical shapes. As can be seen in Fig. 4b, this agglomeration and higher size of the product can be attributed to the nanofibers linkage effect. For example, the particle shown in Fig. 4b is formed by three single particles linked by the CNFs. According to this figure, the CNFs can be found inside the microcapsules or forming bridges between them.

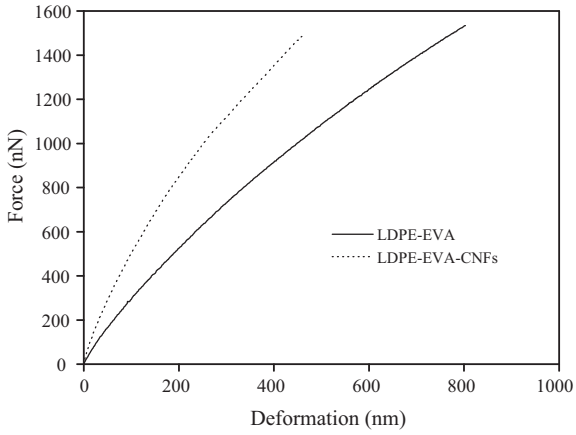

Fig. 5. Mechanical tests performed by AFM. Curves of applied force vs deformation for the microcapsules containing PCMs synthesized by spray drying technique.

3.2. Nanomechanical testing

Fig. 5 shows the mechanical tests performed by AFM technique for the microcapsules containing Rubitherm®RT27 obtained in the laboratory by spray drying with and without CNFs. These mechanical testing results show that a larger force is required to deform microcapsules incorporating CNFs when compared to microcapsules without CNFs. The approximately linear force–deformation behavior exhibited in Fig. 5 indicates an elastic material behavior within the range of forces applied but exhibiting a smooth curvature. The average slopes of the curves for the material with and without CNFs were 2.02 and 3.70 N/m, indicating that the force required to produce the same microcapsule deformation is approximately 183% higher when a 2 wt% of CNFs was added in the microcapsule recipe. According to these results, CNFs addition increases the stiffness and thus the Young's modulus of the microcapsules synthesized by using the spray drying technique.

We note that the displacement of the AFM probe into the microcapsule can either indent the microcapsule or cause compression of the microcapsule from a sphere to an oblated spheroid (a squashed sphere). As the microcapsules have a more rigid but thin shell, resistance to the AFM probe displacement will be initially high but become lower as the displacement increases i.e. the sphere becomes oblate. We see this behavior in Fig. 5, supporting the mechanism of the microcapsule becoming oblate during deformation. Recent work also shows that indentation of a polymer with an AFM probe produces a progressively increasing force with deformation [40]. This previous indentation behavior is opposite to our

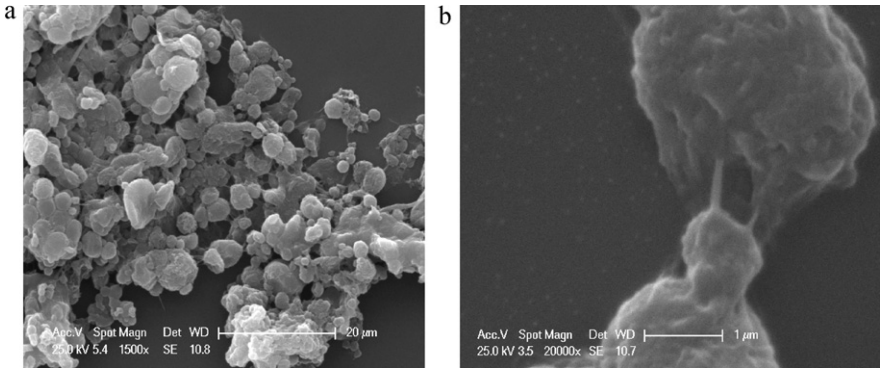

Fig. 4. SEM images of microcapsules of LDPE–EVA containing Rubitherm®RT27 and CNFs, with magnification of a) ×1500 and b) ×20,000, operating in both cases at 25 kV.

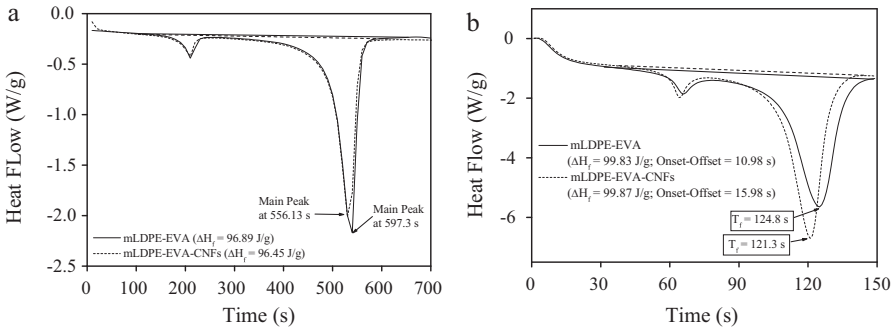

Fig. 6. DSC analyses of microcapsules of LDPE–EVA containing Rubitherm®RT27 with and without CNFs and using a heating rate of 30 °C/min.

observed data in Fig. 5 and highlights how significant AFM probe indentation into the microcapsule does not occur.

3.3. Latent heat

Results of the DSC analyses, peak onset and offset, the main peak (T_f), the TES capacity (ΔH_f) and the paraffin content, are shown in Table 1. As can be seen, microcapsules containing an amount larger than 49% of encapsulated paraffin with a shell from LDPE–EVA can be synthesized by spray drying. This value is similar to that obtained when the same paraffin was microencapsulated from PS shell by suspension polymerization (48.61%). Moreover, the TES capacity of these materials is also comparable with that exhibited by the commercial material Micronal®DS 5001X (116.2 J/g). It was also found that although the CNFs changed the particles morphology and promoted their agglomeration, they did not affect the microencapsulation of the paraffin; since the TES capacity of the microcapsules containing CNFs is really similar to those without them. In the same way, DSC analyses indicated that microcapsules containing only the paraffin Rubitherm®RT27 have similar onset, T_f and offset independently on the shell material. Thus, this scanning rate is slow enough to ensure the thermodynamic equilibrium [41]. In the case of the commercial paraffin, the peak width is larger than those of the microcapsules, what can be attributed to the larger amount of PCM. According to the peak characteristics of the BASF microcapsules, it can be said that the core material is similar to the Rubitherm®RT27. On the other hand, the peak slightly shifts to lower temperature with the addition of CNFs, being narrower than the peak without them. This result can be explained by the high thermal conductivity of CNFs (175–200 W/mK) [34] which is really higher than those of the other microcapsule materials LDPE (0.15–0.543 W/mK) EVA (0.13 W/mK), Rubitherm®RT27 (0.2 W/mK) and PS (0.14–0.18 W/mK) [45–49]. This result agrees with those reported by Salaün [50] who observed an increase in the temperature interval of the phase change when a material of lower conductivity was added to the PCM and also with the reduction in the required time for the phase change observed by Frusteri et al. [34] and Sari and Karaipekli [51] when carbon-fibers and expanded graphite, respectively, were added to PCMs. Hence, the presence of CNFs seems to enhance the thermal conductivity of the composite,

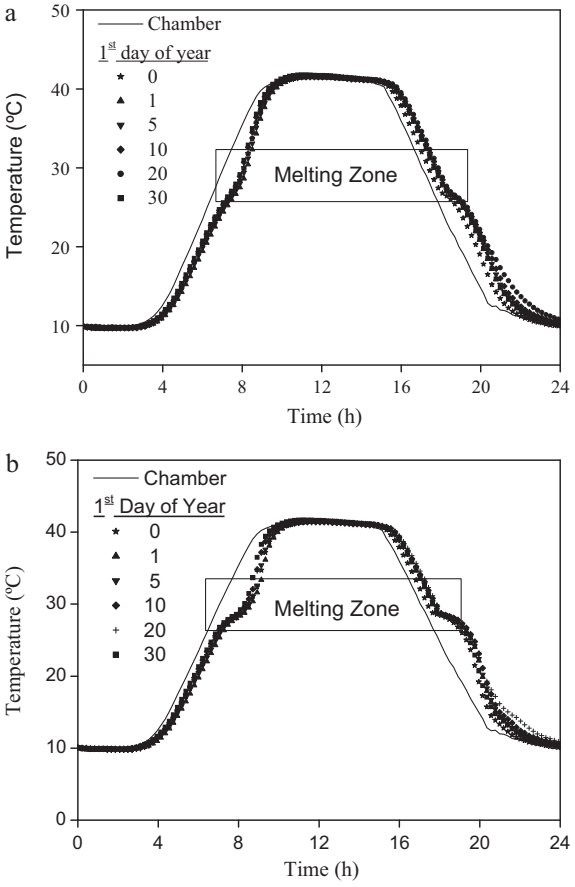

Fig. 7. Thermal stability cycles of microcapsules containing Rubitherm®RT27 using two different shells a) LDPE–EVA and b) polystyrene.

accelerating the energy absorption of the microcapsules. In order to confirm this increase in the thermal conductivity, DSC analyses at a scanning rate of 30 °C/min were carried out.

A comparison between DSC results obtained at heating rates of 5 and 30 °C/min is shown in Fig. 6. As expected, attending to the

Table 1
Paraffin wax and microcapsules thermal data.

Product	Onset (°C)	Offset (°C)	T_f (°C)	ΔH_f (J/g)	Paraffin content (wt%)
Rubitherm®RT27	25.42	31.15	29.41	199	100
m-LDPE–EVA–RT27	25.79	30.25	28.40	98.14	49.32
m-PS–RT27	26.12	30.28	28.46	96.74	48.61
m-BASF	25.28	31.42	27.67	116.2	Unkown
m-LDPE–EVA–RT27-CNFs	25.17	29.45	27.6	95.64	48.06

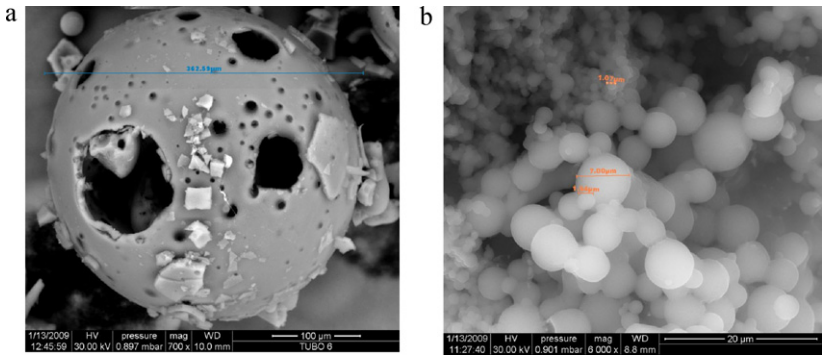

Fig. 8. SEM micrographs of the microcapsules containing Rubitherm®RT27 after 3000 cycles of thermal stability using two different shells a) polystyrene with magnification ×700 and b) LDPE–EVA with magnification ×6000, operating in both cases at 30 kV.

characteristics of material containing PCMs, high latent heat and low thermal conductivity, the temperature of the peak increases with the scanning rate when the analyzed samples have the same mass [41,50]. This figure indicates that when the scanning rate is proper to achieve the thermodynamical equilibrium (Fig. 6a), minimum differences can be found in the peak properties for materials having similar TES capacity. Nevertheless, Fig. 6b confirms that an increase in the scanning rate involves a shift in the peak, increasing the peak temperature. This peak shift was lower for the microcapsules containing CNFs, despite of having similar latent heats, indicating that the higher conductivity of this material promotes a faster heat absorption.

3.4. Thermal stability

The thermal stability cycles of the microcapsules containing paraffin Rubitherm®RT27 obtained by spray drying and suspension polymerization are shown in Fig. 7. The temperature profile inside the glass vial containing microcapsules is different from that of the climatic chamber in the heating or cooling processes. As can be seen in Fig. 7, a slope change was observed in the glass vial temperature profile containing microcapsules when the temperature of the climatic chamber overpassed or underwent the paraffin melting range for heating or cooling processes, respectively. This behavior seems to be more marked for the microcapsules from PS, difference that can be related either by the average particle size or the energy diffusion resistance. According to the SEM micrographs (Fig. 8), the particles size of the microcapsules from PS (360 μm) is really higher than those from LDPE–EVA (3.5 μm), which increases the resistance to the energy transfer. Nevertheless, the lower stability of the PS respect to that of LDPE–EVA exhibited in Fig. 8, in which some fractures appeared on the external surface of these microcapsules after many operating cycles, indicates the paraffin leakage and thus, the temperature profile of this material is not influenced by the thermal resistance of the polymer shell. This way, they work as a non-encapsulated paraffin. This result could be explained by the structure type of the microcapsules, since those from LDPE–EVA form a homogeneous material, considering the paraffin dispersed into the three dimensional netted structure of the polymer [21], whereas microcapsules from PS are initially formed by a core–shell structure [9]. Thus, the high flexibility of the shell formed by polyethylene and EVA polymers avoids the paraffin leakage, regardless the operation time. Thus, the mixture paraffin–polymer works as a unique material, smoothing the thermoregulating action of the PCM during the process.

Finally, the thermal profile exhibited by these two kinds of microcapsules regardless the operating time, confirms the stability of the paraffin Rubitherm®RT27 and the reversibility of this melting process.

4. Conclusions

Spray drying technique can be used to encapsulate the paraffin Rubitherm®RT27 with and without carbon nanofibers (CNFs) using polyethylene–EVA as a polymer shell, exhibiting a high microencapsulation efficiency and avoiding the waste generation. The developed material was homogeneous with a small particle size, having a high heat storage capacity similar to those obtained by suspension polymerization or the commercial Micronal®DS 5001X. Besides, the thermal analysis indicated that it is possible to enhance the thermal conductivity of the microcapsules by the CNFs addition, maintaining the heat storage capacity and increasing the microcapsules stiffness. In this paper, it is also indicated that CNFs can be found inside the microcapsules or forming bridges between them, modifying the final particle size. On the other hand, thermal stability studies carried out over 3000 cycles, indicated that the wax within the synthesized microcapsules melts and solidifies in a reversible way during 30 years of continuous operation time. These microcapsules seemed to be more thermally stable than those formed from PS. The unique problem that presents this procedure is the particle agglomeration that took place into the drying chamber, which can be minimized by using a high stream of gas carrier or decreasing the temperature of the drying chamber to a proper value.

Acknowledgements

Financial support from Acciona Infraestructuras S.A., the fellowship and grant from the Spanish Ministry of Science and Innovation (A.M. Borreguero), are gratefully acknowledged. We are grateful to Ines Jimenez of the Engineering and Material Science Department of Queen Mary University of London for her experimental assistance in the use of AFM equipment.

References

[1] N. Sarier, E. Onder, Thermal characteristics of polyurethane foams incorporated with phase change materials, Thermochim. Acta 454 (2007) 90–98.
[2] H. Mehling, L.F. Cabeza, Heat and Cold Storage with PCM. An up to Date Introduction into Basics and Applications, Springer, Berlin, 2008.
[3] V.V. Tyagi, D. Buddhi, PCM thermal storage in buildings: a state of art, Renew. Sustain. Energy Rev. 11 (2007) 1146–1166.
[4] B. Zalba, J.M. Marín, H.M. Cabeza, Review on thermal energy storage with phase change: materials, heat transfer analysis and applications, Appl. Therm. Eng. 23 (2003) 251–283.
[5] M.M. Farid, A.M. Kuhdhair, S.A.K. Razack, S. Al-Hallaj, A review on phase change energy storage: materials and applications, Energy Convers. Manage. 45 (2004) 1597–1615.
[6] P. Schossig, H.M. Henning, S. Gschwander, T. Haussmann, Microencapsulated phase change materials into construction materials, Sol. Energy Mater. Sol. Cells 89 (2005) 297–306.
[7] A. Sari, A. Karaipekli, C. Alkan, Preparation, characterization and thermal properties of lauric acid/expanded perlite as novel form-stable composite phase change material, Chem. Eng. J. 155 (2009) 899–904.

[8] M.N.A. Hawlader, M.S. Uddin, M.M. Kihn, Microencapsulated PCM thermal-energy storage system, Appl. Energy 74 (2003) 195–202.
[9] L. Sanchez, P. Sanchez, A. de Lucas, M. Carmona, J.F. Rodriguez, Microencapsulation of PCMs with a polystyrene shell, Colloid. Polym. Sci. 285 (2007) 1377–1385.
[10] L. Sánchez, P. Sánchez, M. Carmona, A. de Lucas, J.F. Rodríguez, Influence of operation conditions on the microencapsulation of PCMs by means of suspension-like polymerization, Colloid. Polym. Sci. 286 (2008) 1019–1027.
[11] A.M. Borreguero, M. Carmona, M.L. Sánchez, J.L. Valverde, J.F. Rodríguez, Improvement of the thermal behaviour of gypsum blocks by the incorporation of microcapsules containing PCMs obtained by suspension polymerization with an optimal core/coating mass ratio, Appl. Therm. Eng. 30 (2010) 1164–1169.
[12] L. Sánchez-Silva, J.F. Rodríguez, A. Romero, A.M. Borreguero, M. Carmona, P. Sánchez, Microencapsulation of PCMs with a styrene-methyl methacrylate copolymer shell by suspension-like polymerization, Chem. Eng. J. 157 (2010) 216–222.
[13] J.K. Choi, J.G. Lee, J.H. Kim, H.S. Yang, Preparation of microcapsules containing phase change materials as heat transfer media by in-situ polymerization, J. Ind. Eng. Chem. 7 (2001) 358–362.
[14] J. Su, L. Wang, L. Ren, Fabrication and thermal properties of MicroPCMs: used melamine-formaldehyde resin as shell material, J. Appl. Polym. Sci. 101 (2006) 1522–1528.
[15] J.F. Su, L.X. Wang, L. Ren, Z. Huang, Mechanical properties and thermal stability of double-shell thermal-energy-storage microcapsules, J. Appl. Polym. Sci. 103 (2007) 1295–1302.
[16] H. Zhang, X. Wang, Fabrication and performances of microencapsulated phase change materials based on n-octadecane core and resorcinol-modified melamine-formaldehyde shell, Colloids Surf. A 332 (2009) 129–138.
[17] C. Liang, X. Lingling, S. Hongbo, Z. Zhibin, Microencapsulation of butyl stearate as a phase change material by interfacial polycondensation in a polyurea system, Energy Convers. Manage. 50 (2009) 723–729.
[18] G. Fang, H. Li, F. Yang, X. Liu, S. Wu, Preparation and characterization of nano-encapsulated n-tetradecane as phase change material for thermal energy storage, Chem. Eng. J. 153 (2009) 217–221.
[19] Y. Hong, G. Xin-shi, Preparation of polyethylene–paraffin compound as a form-stable solid–liquid phase change material, Sol. Energy Mater. Sol. Cells 64 (2000) 37–44.
[20] A. Sari, Form-stable paraffin/high density polyethylene composites as solid–liquid phase change material for thermal energy storage: preparation and thermal properties, Energy Convers. Manage. 45 (2004) 2033–2042.
[21] Y. Cai, Y. Hu, L. Song, Q. Kong, R. Yang, Y. Zhang, Z. Chen, W. Fan, Preparation and flammability of high density polyethylene/paraffin/organophilic montmorillonite hybrids as a form stable phase change material, Energy Convers. Manage. 48 (2007) 462–469.
[22] M. Bader, Microencapsulated Paraffin in Polyethylene for Thermal Energy Storage. Capstone Project Report, University of Auckland, New Zealand, 2002.
[23] S.K. Ghosh, Functional Coating: by Polymer Microencapsulation, Wiley–VCH, Weinheim, 2006.
[24] Y. Shin, D. Yoo, K. Son, Development of thermoregulating textile materials with microencapsulated Phase Change Materials (PCM). II. Preparation and application of PCM microcapsules, J. Appl. Polym. Sci. 96 (2005) 2005–2010.
[25] P.C. Gopalratnam, R.P. O'Connor, Spray Dryers. A Guide to Performance Evaluation, second ed., American Institute of Chemical Engineers, New York, 2003.
[26] J.M. Obón, M.R. Castellar, M. Alacid, J.A. Fernández-López, Production of a red-purple food colorant from *Opuntia stricta* fruits by spray drying and its application in food model system, J. Food Eng. 90 (2009) 471–479.
[27] C.M. van't Land, Industrial Drying Equipment: Selection and Application, Marcel Dekker, New York, 1991.
[28] K. Peippo, P. Kauranen, P.D. Lund, A multicomponent PCM wall optimized for passive solar heating, Energy Build. 17 (1991) 259–270.
[29] A. Gharsallaoui, G. Roudaut, O. Chambin, A. Voilley, R. Saurel, Applications of spray-drying in microencapsulation of food ingredients: an overview, Food Res. Int. 40 (2007) 1107–1121.
[30] A. Billon, B. Bataille, G. Cassanas, M. Jacob, Development of spray-dried acetaminophen microparticles using experimental designs, Int. J. Pharm. 203 (2000) 159–168.
[31] V. Fernández-Pérez, J. Tapiador, A. Martín, M.D. Luque de Castro, Optimization of the drying step for preparing a new commercial powdered soup, Innov. Food Sci. Emerg. Technol. 5 (2004) 361–368.
[32] B. Fei, H. Lu, K. Qi, H. Shi, T. Liu, X. Li, J.H. Xin, Multi-functional microcapsules produced by aerosol reaction, J. Aerosol Sci. 39 (2008) 1089–1098.
[33] A. Mills, M. Farid, J.R. Selman, S. Al-Hallaj, Thermal conductivity enhancement of phase change materials using a graphite matrix, Appl. Therm. Eng. 26 (2006) 1652–1661.
[34] F. Frusteri, V. Leonardi, G. Maggio, Numerical approach to describe the phase change of an inorganic PCM containing carbon fibres, Appl. Therm. Eng. 26 (2006) 1883–1892.
[35] W. Wang, X. Yang, Y. Fang, J. Ding, J. Yan, Enhanced thermal conductivity and thermal performance of form-stable composite phase change materials by using β-aluminium nitride, Appl. Energy 86 (2009) 1996–2200.
[36] A. Karaipekli, A. Sari, Preparation, thermal properties and thermal reliability of eutectic mixtures of fatty acids/expanded vermiculite as novel form-stable composites for energy storage, J. Ind. Eng. Chem. 16 (2010) 767–773.
[37] V. Jiménez, P. Sánchez, A. De Lucas, J.L. Valverde, A. Romero, Influence of the nature of the metal hydroxide in the porosity development of carbon nanofibers, J. Colloid Interface Sci. 336 (2009) 226–234.
[38] J. Gravalos, I. Calvo, J. Mieres, J. Cubillo, A.M Borreguero, M. Carmona, J.F Rodriguez, J.L. Valverde, Procedure for microencapsulation of phase change materials by spray drying, Patent EP2119498 (A1) (2009).
[39] A. Elgafy, K. Lafdi, Effect of carbon nanofiber additives on thermal behavior of phase change materials, Carbon 43 (2005) 3067–3074.
[40] W. Wang, A.J. Bushby, A.H. Barber, Nanomechanical thermal analysis of electrospun polymer fibers, Appl. Phys. Lett. 93 (2008) 201907–201910.
[41] M. Mehling, H.P. Ebert, P. Schossig, Development of standards for materials testing and quality control of PCM, in: Proceedings of the 7th IIR Conference on Phase Change Materials and Slurries for Refrigeration and Air Conditioning, France, 2006.
[42] E.S.K. Tang, L. Wang, C.V. Liew, L.W. Chan, P.W.S. Heng, Drying Efficiency and particle movement in coating—impact on particle agglomeration and yield, Int. J. Pharm. 350 (2008) 172–180.
[43] G.É.G. Moreira, M.G.M. Costa, A.C. Rodrigues de Souza, E. Sousa de Brito, M.F.D. de Medeiros, H.M.C. de Azeredo, Physical properties of spray dried acerola pomace extract as affected by temperature and drying aids, LWT Food Sci. Technol. 42 (2009) 641–645.
[44] A.M. Goula, K.G. Adamopoulos, Spray drying of tomato pulp in dehumidified air: I. Effect on the product recovery, J. Food Eng. 66 (2005) 25–34.
[45] A. Greco, A. Maffezzoli, Correction of melting peaks of different PE grades accounting for heat transfer in DSC samples, Polym. Test. 27 (2008) 61–74.
[46] H. Zhang, X. Wang, D. Wu, Silica encapsulation of n-octadecane via sol-gel process: a novel microencapsulated phase change material with enhanced thermal conductivity and performance, J. Colloid Interface Sci. 343 (2010) 246–255.
[47] D. Kumlutas, I.H. Tavman, T.M. Çoban, Thermal conductivity of particle filled polyethylene composite materials, Compos. Sci. Technol. 63 (2003) 113–117.
[48] I. Krupa, V. Cecen, R. Tlili, A. Boudenne, L. Ibos, Thermophysical properties of ethylene-vinylacetate copolymer (EVA) filled with wollastonite fibers coated by silver, Eur. Polym. J. 44 (2008) 3817–3826.
[49] R. Vennix, MATBASE, http://www.matbase.com/material/polymers/commodity.
[50] F. Salaün, E. Devaux, S. Bourbigot, P. Rumeau, P.O. Chapuis, S.K. Saha, S. Volz, Polymer nanoparticles to decrease thermal conductivity of phase change materials, Thermochim. Acta 477 (2008) 25–31.
[51] A. Sari, A. Kraipekli, Thermal conductivity and latent heat thermal energy storage characteristics of paraffin/expanded graphite composite as phase change material, Appl. Therm. Eng. 27 (2007) 1271–1277.